An Online Measurement Method for Noise-Source Impedance of Electrical Equipment

Mingxing Du[1, 2, *], Yang Li[1], Hongbin Wang[2], Ziwei Ouyang[1], and Kexin Wei[1]

Abstract—The paper presents a method of extracting noise source impedance of electrical equipment under working condition. Firstly, based on the theory of two-port network, the measurement method of noise impedance is analyzed theoretically, and the injection probe and receiving probe are calibrated by two known resistors. No special calibration fixture is needed to calibrate the injection probe and receiving probe. Secondly, the port structure of the noise impedance measurement method is analyzed, and the noise source impedance is calculated by using the theory of microwave transmission. Compared with the traditional method, this method does not require calibration fixture and simplifies the experimental process. Finally, passive devices and active systems are tested respectively, and the experimental results show that the method is effective and feasible.

1. INTRODUCTION

Electromagnetic compatibility (EMC) is an important issue for safe and reliable operation of electrical equipment. With the wide application of power devices, the problem of electromagnetic interference (EMI) is becoming more and more serious in power electronic systems. At present, filtering is the main way to suppress the conducted EMI of electrical and electronic equipment and improve its immunity. It is also an important auxiliary measure to ensure the overall or local shielding effectiveness of equipment. EMI filter is a kind of filter commonly used in a power electronic system [1]. Traditional EMI filters generally set the source impedance and load impedance to $50\,\Omega$. This design can make the performance parameters of EMI filters achieve the best under test conditions. However, due to various reasons, the source impedance and load impedance of the equipment cannot guarantee $50\,\Omega$ under the actual working conditions, so the performance of the filter is difficult to achieve the best. Impedance mismatch is a common method to improve the performance of EMI filters [2]. Therefore, it is necessary to study impedance mismatch technology to improve the performance of EMI filters, and measuring and analyzing the internal noise sources impedance is a prerequisite.

Nowadays, there are many methods to measure the noise source impedance. In [3], the equivalent model for off-line converting EMI using resonance method is proposed, and the inductor is added to generate resonance. The equivalent impedance of EMI is derived from the resonant frequency and quality factor. This method is suitable for narrow frequency band. In [4], the insertion loss method is used to measure the noise source impedance. Through series common mode (CM) choke and parallel differential mode (DM) capacitance in the circuit, the CM and DM noises in the circuit are reduced, and the internal noise source impedance in the working state is obtained indirectly by measuring the changes of the noise. However, this method can only be applied to the case where the source impedance is very large or very small. In [5], double current probe method is used to measure the impedance of

noise source. This method can accurately measure its amplitude-frequency characteristics but cannot measure its phase-frequency characteristics. In addition, impedance measurement is also very important in other fields, such as on-line measurement of battery impedance at different frequencies [6–8].

As mentioned earlier, there are many ways to measure impedance, each of which has its application scope or conditions. Therefore, the measurement requirements and conditions, such as measurement frequency band, measurement accuracy, and easy operation, should be taken into account when selecting the method. This paper presents a method of measuring and calculating the noise source impedance of electrical equipment in working condition based on cascaded two-port network transmission matrix and microwave transmission theory. The test method does not need direct electrical contact with the equipment to be tested. It only needs two current probes to clamp the conductors of the equipment to be tested. It is safe for staff and measuring instruments. It only needs to measure several sets of S parameters. Then the noise source impedance can be obtained by simple calculation. The effective bandwidth measured is 1 MHz–100 MHz.

The content of this paper is arranged as follows. The second part analyses the basic principle of the measurement method proposed in this paper. In the third part, passive and active devices are tested respectively, and the feasibility of the proposed method is proved. The fourth part analyses and summarizes the experimental results.

2. MEASURING METHOD

The measuring principle of this method is shown in Fig. 1. The measuring instrument includes an injection current probe, a receiving current probe, and a vector network analyzer (VNA). The whole circuit includes power supply, equipment under test (EUT), and connecting wires. The radio frequency (RF) signal is injected into the circuit from port 1 of VNA through the injection current probe, and the receiving current probe receives the RF signal in the loop to port 2 of VNA. The circuit is powered by power supply VS. It can be an AC or DC source. It can be set up according to the needs of the equipment to be tested. ZX is the impedance of EUT in working condition, ZW the impedance of connecting wires, ZS the impedance of power supply, and Z_{sum} is the sum of the impedance of the loop circuit, which is composed of ZX, ZW, and ZS.
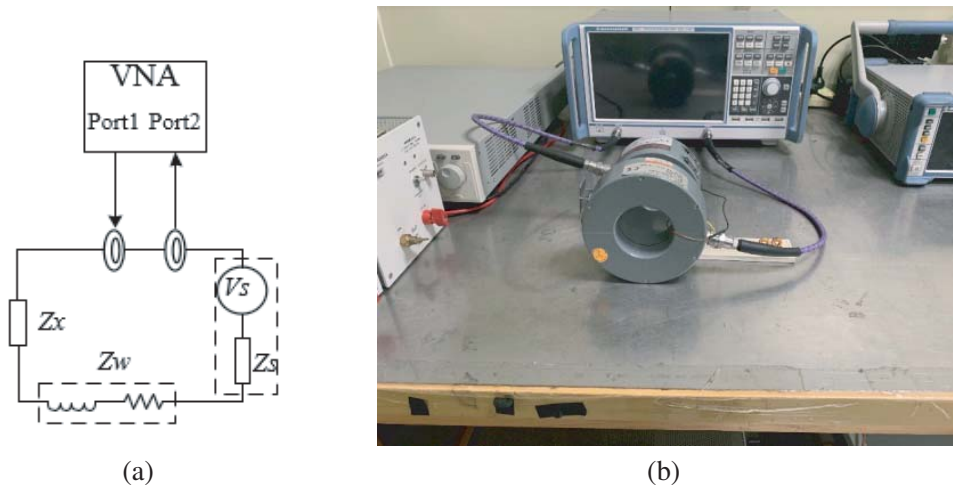
Figure 1. Measurement system. (a) Electrical schematic. (b) System layout.

In fact, the current probe and clamped conductor can be equivalent to a transformer [9] whose turn ratio is $N : 1$, as shown in Fig. 2. The transformer can be represented as a two-port network. One port is the injection current probe or the receiving current probe, and the other port is the two ends of the clamped wire. Therefore, the injection probe, the measurement circuit and receiving probe can be modeled as three cascaded two-port networks as shown in Fig. 3.
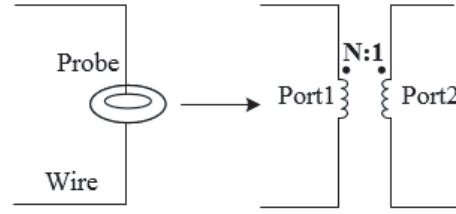
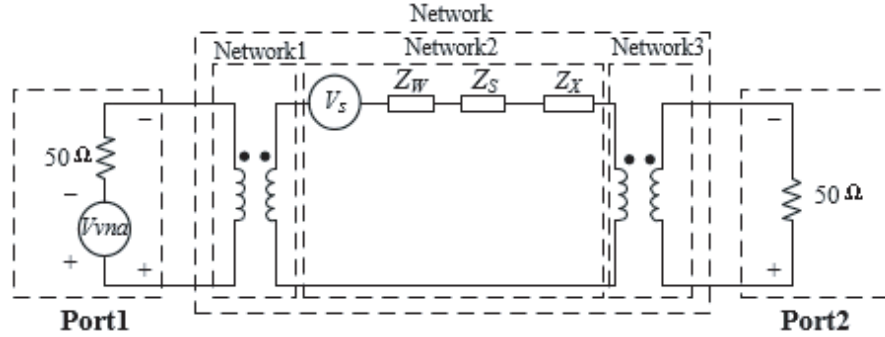**Figure 2.** Equivalent two-port network formed by current probe and clamped wire.
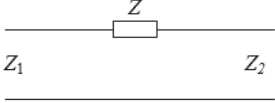

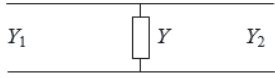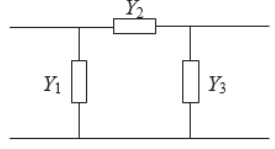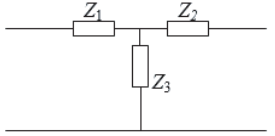**Figure 3.** Equivalent model of measurement system.

Network 1 is a two-port inductive coupling network consisting of injected probe and clamped wire. Network 2 is a two-port network consisting of devices to be measured, power supply, and connecting wire. Network 3 is a two-port inductive coupling network consisting of receiving probe and clamped wire. In Fig. 3, the three networks consist of three cascaded two ports. The transmission matrix of the cascaded two ports has the following relationship:

$$\left[\begin{array}{cc} A & B \\ C & D \end{array}\right] = \left[\begin{array}{cc} A_1 & B_1 \\ C_1 & D_1 \end{array}\right]\left[\begin{array}{cc} A_2 & B_2 \\ C_2 & D_2 \end{array}\right]\left[\begin{array}{cc} A_3 & B_3 \\ C_3 & D_3 \end{array}\right] \tag{1}$$

where $\left[\begin{array}{cc} A & B \\ C & D \end{array}\right]$, $\left[\begin{array}{cc} A_1 & B_1 \\ C_1 & D_1 \end{array}\right]$, $\left[\begin{array}{cc} A_2 & B_2 \\ C_2 & D_2 \end{array}\right]$, $\left[\begin{array}{cc} A_3 & B_3 \\ C_3 & D_3 \end{array}\right]$ represent the transmission matrices of network, network 1, network 2, and network 3, respectively. Because there is a certain relationship between parameter B and impedance in the transmission matrix of network 2 [10], and Z_{sum} in the measurement circuit can be obtained by solving the transmission matrix of network 2. Several models commonly used in network 2 are given in Table 1. The parameters in these transmission matrices have a certain relationship with impedance or admittance. By solving the transmission matrix, impedance or admittance can be obtained. Two-port network and transmission matrix are also used in [11, 12]. These methods have high measurement accuracy. However, they need to make a special calibration fixture to calibrate the transmission matrixes of the injection probe (network 1) and receiving probe (network 3). The manufacturing process of the specific fixture is complex and difficult to operate. The advantage of the method proposed in this paper is that there is no need to make a specific fixture, only the injection probe and receiving probe of the same specification need to be selected, and then the solution can be solved through calculation.

Taking series impedance as an example for analysis and calculation, the series impedance to be measured in network 2 is represented by Z_{sum}. When measuring, the wiring should be as short as possible to reduce the loop impedance. If the experimental circuit is large and the impedance produced by wiring is large, the impedance produced by wiring must be subtracted. In passive experiments, Z_{sum} is the sum of noise source impedance Z_X and wiring impedance Z_w. The wiring impedance Z_w is shown in Fig. 7. In order to obtain the accurate noise source impedance Z_X, the wiring impedance Z_w should be subtracted. In active experiments, Z_{sum} is the sum of Z_X, Z_w, and Z_S. In order to get Z_X, Z_w, and Z_S should be subtracted. When the model in network 2 is series impedance, the parameters in the

Table 1. Relationship between transmission matrix and impedance and admittance of commonly used models.

Series impedance		$\begin{bmatrix} \mathbf{1} & \mathbf{Z} \\ \mathbf{0} & \mathbf{1} \end{bmatrix}$
Parallel admittance		$\begin{bmatrix} 1 & 0 \\ Y & 1 \end{bmatrix}$
π network		$\begin{bmatrix} 1+\dfrac{Y_2}{Y_3} & \dfrac{1}{Y_3} \\ \dfrac{u}{Y_3} & 1+\dfrac{Y_1}{Y_3} \end{bmatrix}$
T network		$\begin{bmatrix} 1+\dfrac{Z_1}{Z_3} & \dfrac{v}{Z_3} \\ \dfrac{1}{Z_3} & 1+\dfrac{Z_2}{Z_3} \end{bmatrix}$

$$u = Y_1 Y_2 + Y_2 Y_3 + Y_1 Y_3, \quad v = Z_1 Z_2 + Z_2 Z_3 + Z_1 Z_3$$

transmission matrix have the following relations: $A_2 = 1$, $B_2 = Z_{\mathrm{sum}}$, $C_2 = 0$, $D_2 = 1$. The input current probe and receiving current probe are of the same specifications, and they are symmetrically connected with the circuit to be measured. In fact, $ABCD$ parameters are measured through the coupling effect of probe and wire. Even if the specifications of current probe are the same, the measured parameters will be slightly different depending on the measurement location. In other words, even if the specifications of current probes are the same, at different positions, $A_1 \neq D_3$, $B_1 \neq B_3$, $C_1 \neq C_3$, $D_1 \neq A_3$. For the sake of simplification, we ignore this slight different and let the following equation hold: $A_1 = D_3$, $B_1 = B_3$, $C_1 = C_3$, $D_1 = A_3$.

$$\begin{bmatrix} A & B \\ C & D \end{bmatrix} = \begin{bmatrix} A_1 C_1 Z_X + B_1 C_1 + A_1 D_1 & A_1^2 Z_X + 2A_1 B_1 \\ C_1^2 Z_X + 2C_1 D_1 & A_1 C_1 Z_X + B_1 C_1 + A_1 D_1 \end{bmatrix} \tag{2}$$

$$B = A_1^2 Z_X + 2A_1 B_1$$
$$C = C_1^2 Z_X + 2C_1 D_1 \tag{3}$$

Each parameter in the transmission matrix has the following relationship with S-parameter [9]. B-parameter and C-parameter can be expressed as:

$$A = \frac{(1 + S_{11})(1 - S_{22}) + S_{12} S_{21}}{2S_{21}}, \quad B = Z_0 \frac{(1 + S_{11})(1 + S_{22}) - S_{12} S_{21}}{2S_{21}}$$
$$C = \frac{1}{Z_0} \frac{(1 - S_{11})(1 - S_{22}) - S_{12} S_{21}}{2S_{21}}, \quad D = \frac{(1 - S_{11})(1 + S_{22}) + S_{12} S_{21}}{2S_{21}} \tag{4}$$

Two known impedances, Z_{K1} ($1000\,\Omega$) and Z_{K2} ($10\,\Omega$), are connected to the measurement circuit respectively, and the unknown equipment is replaced by Z_X. Then the B-parameter of the network transmission matrix of the whole cascaded network can be expressed as:

$$\begin{cases} B_{Z_{K1}} = A_1^2 Z_{K1} + 2A_1 B_1 \\ B_{Z_{K2}} = A_1^2 Z_{K2} + 2A_1 B_1 \end{cases} \tag{5}$$

where $B_{Z_{K1}}$ and $B_{Z_{K2}}$ are B-parameters of the whole network after cascading when connecting Z_{K1} and Z_{K2}, respectively. In Eq. (5), A_1 parameter of the network 1 transmission matrix can be obtained. $B_{Z_{K1}}$ and $B_{Z_{K2}}$ can be calculated by Eq. (4), and S parameters can be measured by VNA.

$$A_1 = \pm\sqrt{\frac{B_{Z_{K1}} - B_{Z_{K2}}}{Z_{K1} - Z_{K2}}} \tag{6}$$

There are two solutions in Eq. (6). We should take the solution whose real part is greater than 0, because if parameter A of the negative real part is used, the real part of the impedance calculated will be negative, which is not in conformity with the actual situation, so we choose the solution of the positive real part. Add the two equations in Eq. (5) and substitute the calculated parameter A_1 into them to get the B_1 parameter of the network 1 transmission matrix.

$$B_1 = \frac{(B_{Z_{K1}} + B_{Z_{K2}}) - A_1^2(Z_{K1} + Z_{K2})}{4A_1} \tag{7}$$

Similarly, C_1 and D_1 parameters of network 1 transmission matrix can be obtained:

$$C_1 = \pm\sqrt{\frac{C_{Z_{K1}} - C_{Z_{K2}}}{Z_{K1} - Z_{K2}}}$$
$$D_1 = \frac{(C_{Z_{K1}} + C_{Z_{K2}}) - C_1^2(Z_{K1} + Z_{K2})}{4C_1} \tag{8}$$

where $C_{Z_{K1}}$ and $C_{Z_{K2}}$ are the C parameters of the whole network after cascading when connecting Z_{K1} and Z_{K2}, respectively. $C_{Z_{K1}}$ and $C_{Z_{K2}}$ can be calculated by Eq. (4), and S-parameters can be measured by VNA.

After the above calculation, the transmission matrices of network 1 and network 3 are obtained, which are expressed by T_1 and T_3. T is used to represent the transmission matrix of the whole cascade network, and T_2 is used to represent the transmission matrix of network 2, so $T = T_1 T_2 T_3$, $T_2 = T_1^{-1} T T_3^{-1}$, T_1^{-1} and T_3^{-1} represent the inverse matrices of T_1 and T_3, respectively.

Current probes are affected by current variations at different locations, and their operating characteristics may vary. Therefore, a constant power supply should be selected for each experiment, and the experiment time should be minimized to avoid the impact of current changes. If the test position must be replaced, and the current change is obvious. It is necessary to recharacterize the $ABCD$ matrix of the injection probe and the receiving probe to reduce the experimental error.

## 3. EXPERIMENTAL VERIFICATION

3.1. Passive Device Experiments

The color ring resistors of $20\,\Omega$, $68\,\Omega$, $470\,\Omega$, $750\,\Omega$, $1000\,\Omega$, capacitors of $10\,\mathrm{pF}$, $20\,\mathrm{pF}$, and two inductive loads are selected as unknown components to be measured. The measured circuit impedance is the sum of the series impedance of the system and the wire under test.

These passive devices are measured by a precision impedance analyzer. Then, the impedance measured by the proposed method is compared with that measured by precision impedance analyzer. The results are shown in Fig. 4, Fig. 5, and Fig. 6. As shown in Fig. 4, Fig. 5, and Fig. 6, the impedances measured by the proposed method and impedance analyzer are basically in agreement within $100\,\mathrm{MHz}$. There are only some differences at individual frequencies, which may be acceptable in theory due to experimental errors and calculations.

The impedance of the connecting wire and circuit board within $100\,\mathrm{MHz}$ is measured by the proposed method. Due to resonance, a peak occurs at $95\,\mathrm{MHz}$, where the impedance is $144\,\Omega$. Due to bad contact between breadboard and wire, the impedance of the whole frequency band is too large to be neglected. Therefore, we must take this into account. It is necessary to subtract this part of the impedance and draw the measurement results in Fig. 7.
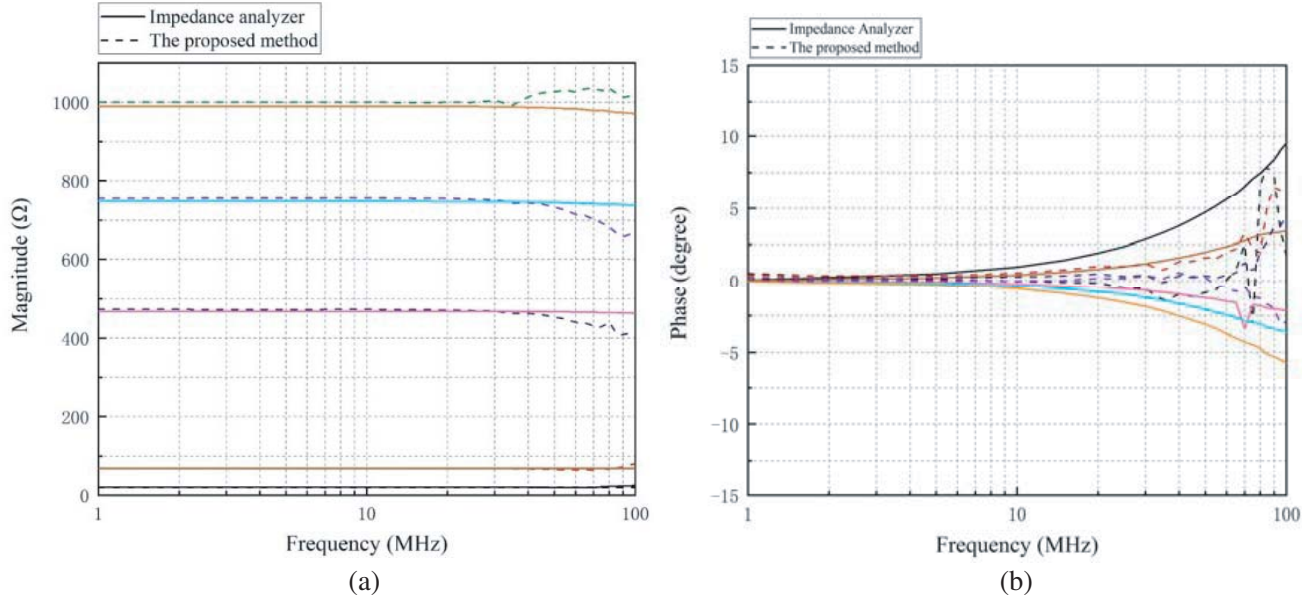
Figure 4. Measurement results of different resistance values. (a) Amplitude. (b) Phase.
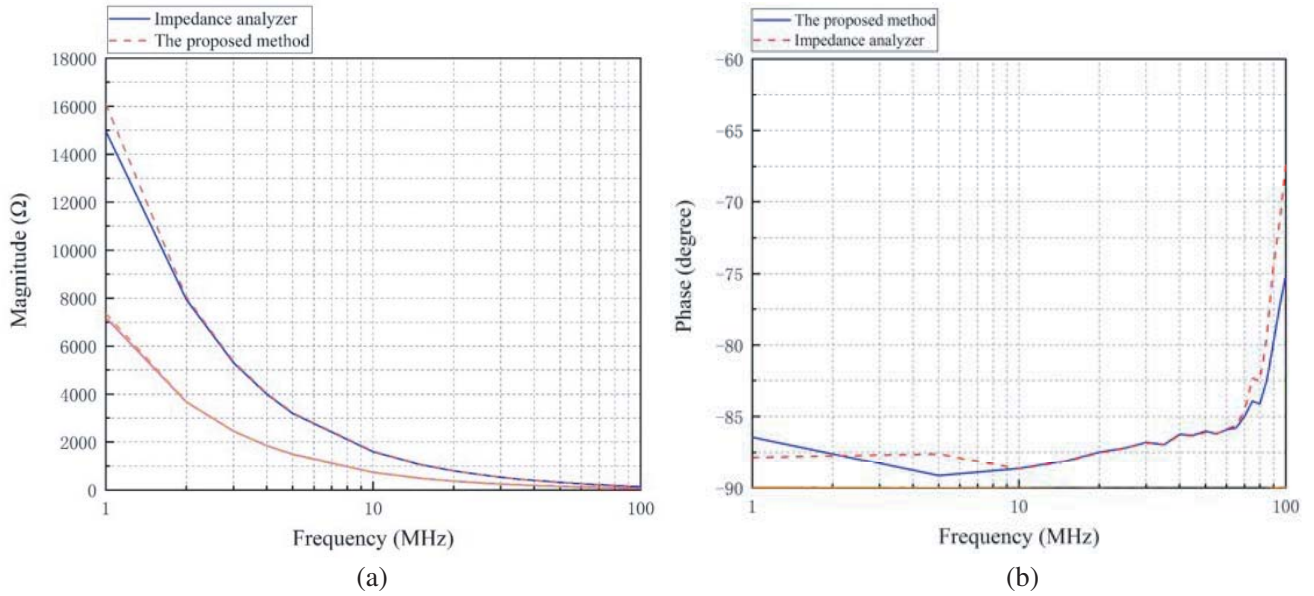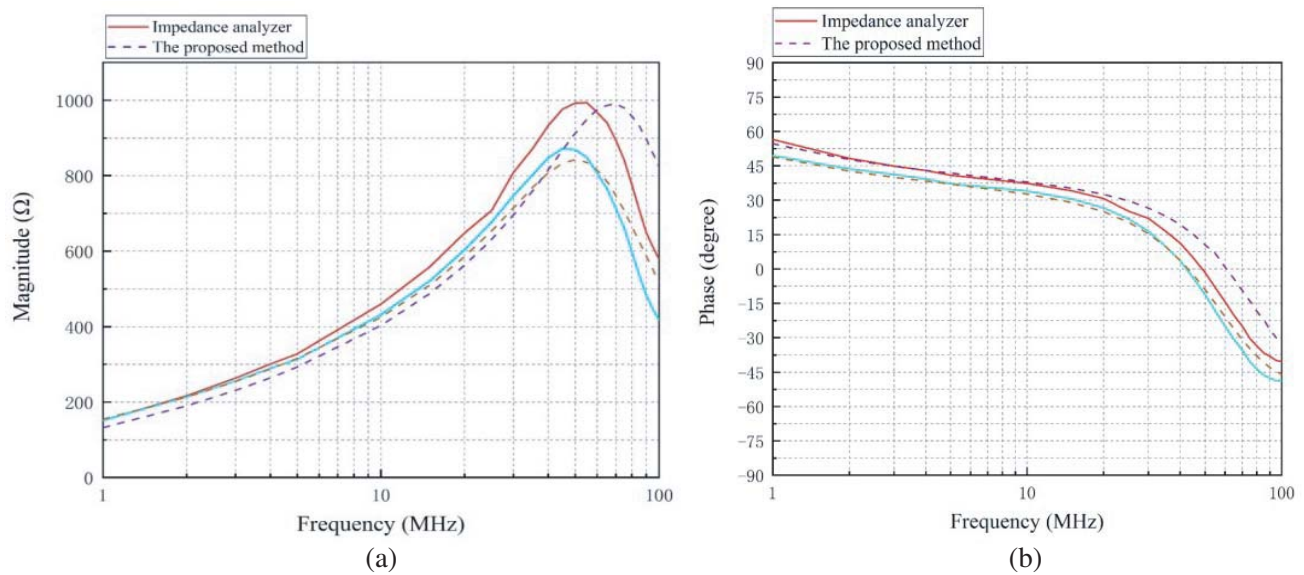

Figure 5. Measurement results for different capacitors. (a) Amplitude. (b) Phase.

3.2. Active Device Experiments

In order to prove the effectiveness of the presented method in circuit impedance measurement, an asynchronous motor used for small electric fan is selected as DUT. The motor is powered by a programmable AC power supply whose model is GWINSTEK aps-7100, and the power supply voltage is 220 V. This experiment is divided into three working states. The first state is measured in the case of no power supply, the second state measured in the 1st gear of the fan, and the third state measured in the 2nd gear of the fan. The second state motor operates at a lower speed and the third at a higher speed.

As shown in Fig. 8, the motor is connected to the AC power supply with two conductors, each

Figure 6. Measurement results for different inductive loads. (a) Amplitude. (b) Phase.
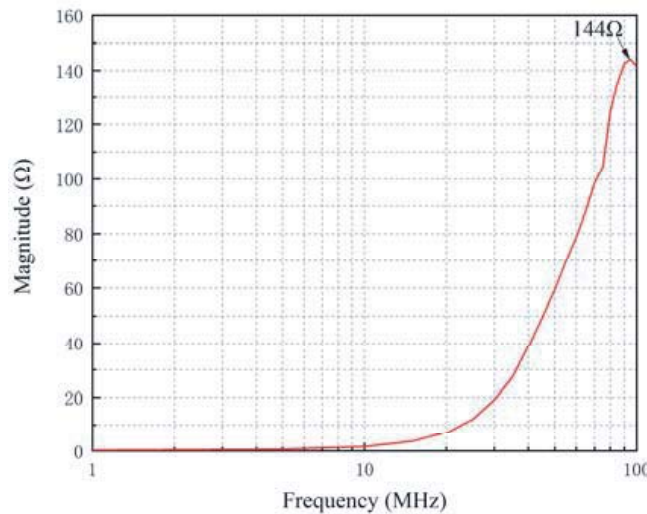

Figure 7. Impedance of connecting conductor and circuit board measured by the proposed method.

10 cm long. The RF signal from port 1 of VNA is coupled to the circuit by an injection probe and then received by the receiving probe back to port 2 of VNA. Based on the analysis in the previous section, we have calculated the transmission matrices of network 1 and network 3 at each frequency point. Therefore, we only need to calculate transmission matrices of the network after the asynchronous motor cascades in three working states. Then, the impedance of these three states can be calculated.

In order to verify the correctness of the experimental results, the method in [13–15] is applied for comparison, and the measured results are shown in Fig. 9. In Fig. 9, the solid line is the measurement result of the proposed method, and the dotted line is the measurement result employing the method mentioned in [13–15]. We can see from Fig. 9 that the results of the two methods basically coincide. Therefore, the correctness of the proposed method is proved. In addition, we can see from Fig. 9 that the impedance of the motor when it is not running is obviously greater than that when it is running.

(a)

(b)
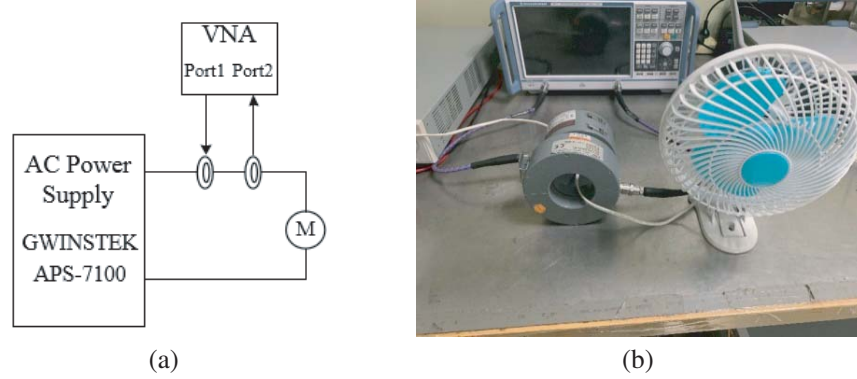
Figure 8. Measuring device of asynchronous motor in operation: (a) electrical schematic; (b) system layout.
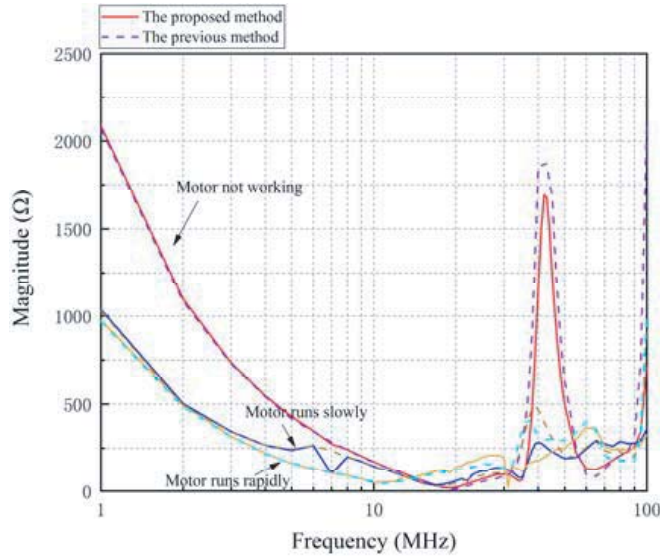
Figure 9. Impedance amplitudes measured by the proposed method and previous methods.

4. CONCLUSIONS

Based on the theory of two-port network and microwave transmission, this paper presents a method of accurately extracting circuit impedance of electrical equipment in operation. Compared with the existing measurement methods, the method proposed in this paper does not need to make a specific calibration fixture to represent the transmission matrix of the injection probe and receiving probe. The transmission matrix of the injection current probe and receiving current probe can be obtained by simply calculating each frequency point. We measure different resistors, capacitors, and inductance loads. Comparing the calculated results with those measured by precision impedance analyzer, the two curves show good consistency. Finally, we measure the asynchronous motor in the running state and then compare the calculated results with those obtained by the existing methods. The two curves also show good consistency, which proves the feasibility of this method.

REFERENCES

1. Han, D., S. Li, Y. Wu, W. Choi, and B. Sarlioglu, "Comparative analysis on conducted CM EMI emission of motor drives," *IEEE Transactions on Industrial Electronics*, Vol. 64, No. 10, 8353–8363, 2017.

2. Zheng, F., W. Wang, X. Zhao, M. Cui, Q. Zhang, and G. He, "Identifying electromagnetic noise-source impedance using hybrid of measurement calculation method," *IEEE Transactions on Power Electronics*, Vol. 34, No. 10, 9609–9618, 2019.

3. Schneider, L. M., "Noise source equivalent circuit model for off-line converters and its use in input filter design," *1983 IEEE International Symposium on Electromagnetic Compatibility*, 167–175, 1983.

4. Zhang, D., D. Y. Chen, M. J. Nave, and D. Sable, "Measurement of noise source impedance of off-line converters," *IEEE Transactions on Power*, Vol. 15, No. 5, 820–825, 2000.

5. See, K. Y. and J. Deng, "Measurement of noise source impedance of SMPS using a two probes approach," *IEEE Transactions on Power Electronics*, Vol. 19, No. 3, 862–868, 2004.

6. Howey, D. A., P. D. Mitcheson, V. Yufit, G. J. Offer, and N. P. Brandon, "Online measurement of battery impedance using motor controller excitation," *IEEE Transactions on Vehicular Technology*, Vol. 63, No. 6, 2557–2566, 2014.

7. Huang, W. and J. A. A. Qahouq, "An online battery impedance measurement method using DC-DC power converter control," *IEEE Transactions on Industrial Electronics*, Vol. 61, No. 11, 5987–5995, 2014.

8. Qahouq, J. A. A., "Online battery impedance spectrum measurement method," *2016 IEEE Applied Power Electronics Conference and Exposition (APEC)*, 3611–3615, 2016.

9. Hu, B., V. Tarateeraseth, K. Y. See, and Y. Zhao, "Assessment of electromagnetic interference suppression performance of ferrite core power cord," *IET Science, Measurement & Technology*, Vol. 4, No. 4, 229–236, Jul. 2010.

10. Pozar, D. M., *Microwave Engineering*, Wiley, Hoboken, NJ, USA, 2009.

11. Li, K. R., K. Y. See, and X. M. Li, "Inductive coupled in-circuit impedance monitoring of electrical system using two-port ABCD network transactions on instrumentation and measurement," Vol. 64, No. 9, 2489–2495, 2015.

12. Li, K. R. and K. Y. See, "Evaluation of conducted EMI measurement without LISN using two-port ABCD network approach for EMI filter design under real operating condition," *2015 Asia-Pacific Symposium on Electromagnetic Compatibility (APEMC)*, 632–635, 2015.

13. Tarateeraseth, V., B. Hu, K. Y. See, and F. G. Canavero, "Accurate extraction of noise source impedance of an SMPS under operating conditions," *IEEE Transactions on Industrial Electronics*, Vol. 25, No. 1, 111–117, 2010.

14. Tarateeraseth, V., "EMI filter design: Part II: Measurement of noise source impedances," *IEEE Electromagnetic Compatibility*, Vol. 1, No. 1, 42–49, 2012.

15. Zhao, B., M. Zhao, Z. Feng, L. Shui, and M. Yao, "An improved dual-probe approach to measure noise source impedance," *2010 Asia-Pacific International Symposium on Electromagnetic Compatibility*, 214–217, 2010.